



Cite this: *Dalton Trans.*, 2019, **48**, 16853

Received 5th September 2019,
Accepted 22nd October 2019

DOI: 10.1039/c9dt03587g

rsc.li/dalton

Complete post-synthetic modification of a spin crossover complex†

Alejandro Enríquez-Cabrera,^{id} Lucie Routaboul, Lionel Salmon^{id}* and Azzedine Bousseksou*

The post-synthetic reaction between *p*-anisaldehyde and the spin-crossover compound $[\text{Fe}(\text{NH}_2\text{-trz})_3](\text{NO}_3)_2$ was explored, obtaining different degrees of transformation from 23% to full conversion by varying the reaction time. The post-synthetic SCO complexes obtained were studied by magnetometry, powder X-ray diffraction (PXRD), elemental analysis, solid state NMR and IR and compared with the corresponding compounds obtained by direct synthetic routes, revealing new spin crossover properties.

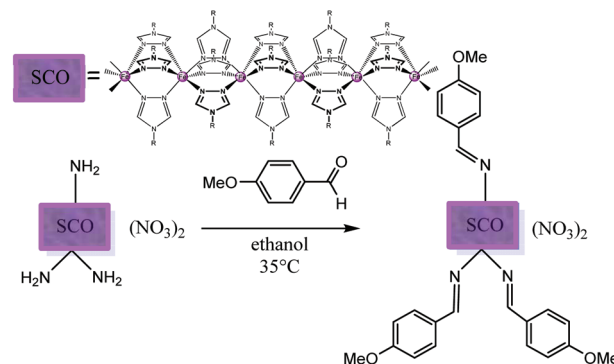
SCO materials have attracted much attention in the past few years due to their integration into different devices¹ for different applications in photonics,² electronics^{3,4} and mechanics.⁵ In order to develop such applications, specific SCO behaviour or transition temperatures are expected, while particular attention is paid to the nanostructuring of the SCO materials.^{6,7} The post-synthetic modification (PSM) involving the chemical transformation or exchange of pre-synthesised materials has emerged as a powerful strategy to introduce a functionality without affecting the original structure. In particular, such a method has proved to be very useful in the recent development of metal-organic frameworks (MOFs)⁸ or biomolecules⁹ and therefore it could be a good approach for the development of new SCO materials.

There are only a few reports concerning PSM and spin crossover materials, dealing with the functionalization of 3D Hofmann clathrate MOFs¹⁰ or chain-like iron-triazole complexes^{11,12} and more recently of a dinuclear iron(III) complex¹³ and $\text{Fe}^{\text{II}}[\text{M}^{\text{IV}}(\text{CN})_8]^{4-}$ ($\text{M} = \text{Mo}, \text{Nb}$) cyanido-bridged frameworks.¹⁴ To the best of our knowledge, no complete reaction has been reported in spite of stoichiometric conditions. Wang *et al.* have recently^{11,12} reported a post-synthetic procedure in which they obtained up to 15% chemical transformation in the final iron-triazole complex, leading to a slight

increase of the spin crossover temperature and new luminescence properties.

In the present paper, we wanted to demonstrate that this post chemical transformation can be fully achieved and can generate spin crossover compounds whose physical properties can be different in comparison with those of the corresponding complexes synthesized by direct methods, opening the way towards new routes for SCO materials.

In order to integrate such materials into devices it is necessary that they undergo a transition above room temperature, for which we started with the complex $[\text{Fe}(\text{NH}_2\text{-trz})_3](\text{NO}_3)_2$ (**1** with $\text{NH}_2\text{-trz} = 4\text{-amino-1,2,4-triazole}$) which in our case has $T_{1/2\uparrow} = 308 \text{ K}$ and $T_{1/2\downarrow} = 338 \text{ K}$. Under the experimental conditions (see the ESI†), the post-synthetic methodology developed in this work leads to the formation of a Schiff base by the reaction of **1** with 12 eq. of *p*-anisaldehyde in ethanol at 35 °C upon increasing the time: 3 h (**2**), 6 h (**3**), 12 h (**4**) and 72 h (**5**) (Scheme 1). The final products were analysed by IR to confirm the presence of imine by its signature peak at 1604 cm^{-1} ($\text{C}=\text{N}$), and the amount of substitution was determined by elemental analyses resulting in 23.2% (**2**), 58.6% (**3**), 78.5% (**4**) and 100% (**5**). It is interesting to notice that an analogous functionalization reaction in 1,2-dichloroethane was unsuccessful, leading instead to the decomposition/oxidation of the



Scheme 1 The post-synthetic reaction using *p*-anisaldehyde.

LCC, CNRS, 205 route de Narbonne, 31077 Toulouse, France.

E-mail: lionel.salmon@lcc-toulouse.fr

† Electronic supplementary information (ESI) available. See DOI: 10.1039/C9DT03587G

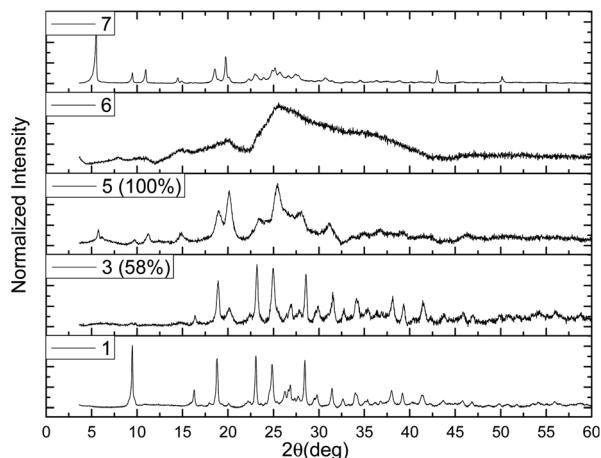


Fig. 1 The powder X-ray diffractograms of samples 1, 3, 5, 6 and 7.

coordination polymer. This shows that the choice of solvent is an important factor in post-synthetic reactions.

We also synthesized the corresponding imino complex by direct synthesis (DS) starting from the imino ligand (see the ESI†) in order to compare its properties with those of the post-synthetic imino complex. It is well known that SCO behaviour is strongly dependent on different structural factors such as crystallinity¹⁵ and polymorphism.¹⁶ Interestingly, we found that in contrast to the post synthetic reaction, the direct synthesis of the imino complex when carried out under normal stirring conditions resulted systematically in an amorphous powder (6); it was necessary to use a solvent diffusion technique in order to obtain a crystalline powder (7) as shown in Fig. 1, and this is important in order to establish a fair structure–property relationship.

The PXRD data for the post-synthetic samples (see the ESI†) reveal that the structure changes while increasing the amount of imine; at 23%, the diffractogram remains nearly the same as that of the amino derivative, while for higher transformations, we can clearly see an additional diffraction pattern. In fact, as considered by Wang *et al.*,¹² the retention of the structure is obtained for weak substitution, which could be considered as grafting. It is interesting to notice that such behaviour is in contrast to that observed for the $[\text{Fe}(\text{Htrz})_2(\text{trz})](\text{BF}_4)$ derivative for which a drastic modification of the structure was observed for only 3% substitution of the triazole ligand by the aminotriazole ligand.¹⁷ In the latter case, the effect on the crystal lattice was attributed to the reorganization of the interactions between the Fe–triazole chains, which are directly linked through N–H...N interactions involving Htrz and trz ligands in the pristine compound.¹⁸ Finally, in the present case, when 100% substitution is achieved the structure is completely modified and is similar to that obtained for the crystalline sample 7. These measurements confirm the complete post synthetic modification and are in agreement with the magnetic measurements reported hereafter which clearly show the presence of two species only for the partially substituted samples.

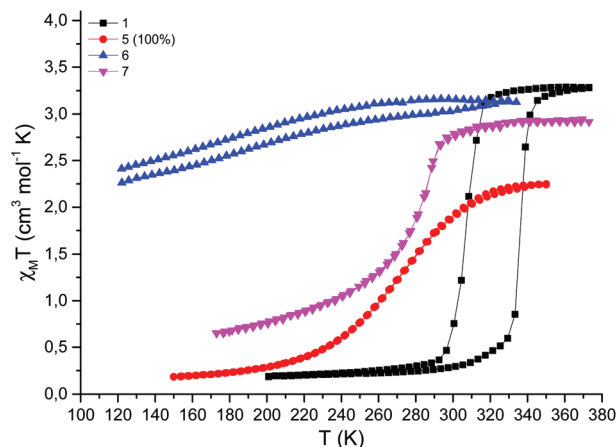


Fig. 2 Magnetic measurements for samples 1, 5, 6 and 7.

Temperature dependent magnetic measurements carried out for samples 1 and 5–7 are shown in Fig. 2 (see the ESI† for other measurements). For each sample we considered the second thermal cycle, the first one corresponding to the desolvation/‘run-in’ cycle. The SCO behaviour depends on the synthetic method used (see Scheme S0†). In comparison with the parent amino derivative the transition is less cooperative and shifted to lower temperature with $T_{1/2} = 278$ K and 287 K for 5 and 7, respectively, while a very incomplete conversion is observed for 6. In the case of the post synthetic method, the completeness of the transition decreases with the transformation rate (see S12†). Such an effect is also observed to a lesser extent for sample 7. In fact, although the general chain architecture of the structure is maintained in all samples as demonstrated by the PXRD study, the synthetic approach implemented plays a key role in the final spin crossover properties. For sample 5, we can suggest that the difficulty in incorporating a bulky moiety into the ligand by the network modifies the inter-chain interactions and steers the molecular network to form a specific packing arrangement.

Regarding the thermal variation of susceptibility as a function of the degree of transformation (see Fig. S13†), it appears that all the intermediate transformations lead to a mixture of two independent complexes. It is interesting to notice that the experiments were repeated twice and led to the same result (the same composition and properties under the same experimental conditions). One explanation could be the presence of domains (core of the powder grains) that remain with the same magnetic properties as the starting amino derivative 1 and other growing domains on the surface of the grains that are transformed into the imine derivative. This hypothesis is in agreement with the fact that the starting complex 1 is insoluble under our experimental conditions. This trend is totally different compared to that obtained for the direct synthesis in the presence of a mixture of ligands (amino and imino ligands). In the latter case, the pace of the SCO curve with only one singularity is consistent with the homogeneous distribution of the imine ligand (see Fig. S14†).

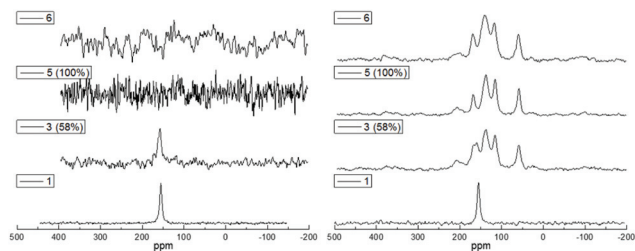


Fig. 3 ^{13}C CP-MAS (left) and ^{13}C MAS (right) NMR spectra of samples 1, 3, 5 and 6.

In order to probe the composition of the samples in depth, we used Mössbauer spectroscopy and NMR spectroscopy, the latter being rarely used to characterize paramagnetic SCO materials. ^{13}C CP-MAS and ^{13}C MAS NMR are two different techniques used to obtain the NMR spectra in the solid state; while the first is adapted for diamagnetic systems, the latter permits us to study also the paramagnetic entities that are associated with faster nuclei relaxation.^{19,20} Indeed, in the ^{13}C CP-MAS spectra at room temperature (Fig. 3), we only observe a peak at 155 ppm corresponding to the triazole core for samples 1–4. Although the intensities of the peaks seem to be similar due to an increase in the number of scans (to observe the peaks, see the ESI†), they decrease from sample 1 to sample 4 in accordance with the increase of susceptibility. Indeed, from the magnetic behaviour observed in Fig. 2, it is clear that at room temperature (heating mode) 1 is diamagnetic, and this characteristic is lost with the degree of transformation (Fig. S13†), explaining the decrease in the intensity of the ^{13}C CP-MAS peak. Moreover, the difficulty in obtaining a signal for sample 5 is in agreement with the majority of HS fractions. In this case, we cannot detect ^{13}C spins in the direct vicinity of the paramagnetic species, which are certainly severely broadened to be indistinguishable from the baseline.²¹ As expected sample 6 is also silent as it is fully paramagnetic. Mössbauer data were collected for sample 5 at 80 and 325 K and confirmed the residual LS fraction at high temperature suspected by magnetic measurements (see the ESI†).

The ^{13}C MAS NMR (Fig. 3) spectrum at room temperature confirms the diamagnetic entities for 1, while the introduction of the imine ligand leads to the appearance of new peaks at 59 ppm (OCH_3), 115 and 137 ppm (aromatic carbons of *p*-anisaldehyde), 169 ppm (triazole core) and 200 ppm ($\text{CH}=\text{N}$) attributed to the paramagnetic species that increase in intensity in agreement with the degree of transformation. Clearly, in contrast to the ^{13}C CP-MAS experiment, ^{13}C MAS NMR allows for the study of the whole system in all cases.

In conclusion, by modifying the reaction time it was possible to obtain a complete post synthetic transformation for a spin crossover complex. The as-obtained Schiff base bearing complex presents different spin crossover properties in comparison with those synthesized by direct methods. Of course, whatever the route used, crystallinity plays a key role in the final behaviour as demonstrated by the comparison of the SCO properties of the two complexes synthesized by different direct

methods. Nevertheless, clearly the post synthetic approach leads to a specific molecular arrangement and physical properties and opens up the way towards the preparation of new SCO complexes. The methodology used in this work is currently under investigation to determine the synergetic effect between SCO and different physical or chemical properties that cannot be accessed through the direct synthetic methodology.

Conflicts of interest

There are no conflicts to declare.

Acknowledgements

A. E.-C. thanks the CONACyT (Mexico) for the postdoctoral grant. We thank Yannick Coppel for NMR measurements and discussions.

Notes and references

- G. Molnár, S. Rat, L. Salmon, W. Nicolazzi and A. Bousseksou, *Adv. Mater.*, 2018, **30**, 1–23.
- C. M. Quintero, I. A. Gural'skiy, L. Salmon, G. Molnár, C. Bergaud and A. Bousseksou, *J. Mater. Chem.*, 2012, **22**, 3745–3751.
- V. Shalabaeva, K. Ridier, S. Rat, M. D. Manrique-Juarez, L. Salmon, I. Séguy, A. Rotaru, G. Molnár and A. Bousseksou, *Appl. Phys. Lett.*, 2018, **112**, 013301.
- J. Dugay, M. Aarts, M. Gimenez-Marqués, T. Kozlova, H. W. Zandbergen, E. Coronado and H. S. J. Van Der Zant, *Nano Lett.*, 2017, **17**, 186–193.
- M. D. Manrique-Juarez, F. Mathieu, V. Shalabaeva, J. Cacheux, S. Rat, L. Nicu, T. Leïchlé, L. Salmon, G. Molnár and A. Bousseksou, *Angew. Chem., Int. Ed.*, 2017, **56**, 8074–8078.
- L. Salmon and L. Catala, *C. R. Chim.*, 2018, **21**, 1230–1269.
- T. Mallah and M. Cavallini, *C. R. Chim.*, 2018, **21**, 1270–1286.
- Z. Yin, S. Wan, J. Yang, M. Kurmoo and M. H. Zeng, *Coord. Chem. Rev.*, 2019, **378**, 500–512.
- S. H. Weisbrod and A. Marx, *Chem. Commun.*, 2008, 5675–5685.
- J. E. Clements, J. R. Price, S. M. Neville and C. J. Kepert, *Angew. Chem., Int. Ed.*, 2014, **53**, 10164–10168.
- C. F. Wang, R. F. Li, X. Y. Chen, R. J. Wei, L. S. Zheng and J. Tao, *Angew. Chem., Int. Ed.*, 2015, **54**, 1574–1577.
- C. F. Wang, G. Y. Yang, Z. S. Yao and J. Tao, *Chem. – Eur. J.*, 2018, **24**, 3218–3224.
- Y. Komatsumaru, M. Nakaya, F. Kobayashi, R. Ohtani, M. Nakamura, L. F. Lindoy and S. Hayami, *Z. Anorg. Allg. Chem.*, 2018, **644**, 729–734.

- 14 S. Kawabata, S. Chorazy, J. J. Zakrzewski, K. Imoto, T. Fujimoto, K. Nakabayashi, J. Stanek, B. Sieklucka and S. I. Ohkoshi, *Inorg. Chem.*, 2019, **58**, 6052–6063.
- 15 A. Grosjean, N. Daro, S. Pechev, C. Etrillard, G. Chastanet and P. Guionneau, *Eur. J. Inorg. Chem.*, 2018, **2018**, 429–434.
- 16 S. Rat, K. Ridier, L. Vendier, G. Molnár, L. Salmon and A. Bousseksou, *CrystEngComm*, 2017, **19**, 3271–3280.
- 17 M. Piedrahita-Bello, K. Ridier, M. Mikolasek, G. Molnár, W. Nicolazzi, L. Salmon and A. Bousseksou, *Chem. Commun.*, 2019, **55**, 4769–4772.
- 18 A. Grosjean, P. Négrier, P. Bordet, C. Etrillard, D. Mondieig, S. Pechev, E. Lebraud, J. F. Létard and P. Guionneau, *Eur. J. Inorg. Chem.*, 2013, **2**, 796–802.
- 19 M. Bertmer, *Solid State Nucl. Magn. Reson.*, 2017, **81**, 1–7.
- 20 N. P. Wickramasinghe, M. A. Shaibat, C. R. Jones, L. B. Casabianca, A. C. De Dios, J. S. Harwood and Y. Ishii, *J. Chem. Phys.*, 2008, **128**, 052210.
- 21 A. V. Kuttatheyil, D. Lässig, J. Lincke, M. Kobalz, M. Baias, K. König, J. Hofmann, H. Krautscheid, C. J. Pickard, J. Haase and M. Bertmer, *Inorg. Chem.*, 2013, **52**, 4431–4442.